JOURNAL OF VIROLOGY, Dec. 2011, p. 13027–13037 Vol. 85, No. 24
0022-538X/11/$12.00 doi:10.1128/JVI.06191-11


# VPg-Primed RNA Synthesis of Norovirus RNA-Dependent RNA Polymerases by Using a Novel Cell-Based Assay▽

Chennareddy V. Subba-Reddy,[1] Ian Goodfellow,[2]* and C. Cheng Kao[1]*

*Department of Molecular and Cellular Biochemistry, Indiana University, Bloomington, Indiana 47405,[1] and Section of Virology, Department of Medicine, Imperial College London, London W2 1PG, United Kingdom[2]*

Received 31 August 2011/Accepted 4 October 2011

**Molecular studies of human noroviruses (NoV) have been hampered by the lack of a permissive cell culture system. We have developed a sensitive and reliable mammalian cell-based assay for the human NoV GII.4 strain RNA-dependent RNA polymerase (RdRp). The assay is based on the finding that RNAs synthesized by transiently expressed RdRp can stimulate retinoic acid-inducible gene I (RIG-I)-dependent reporter luciferase production via the beta interferon promoter. Comparable activities were observed for the murine norovirus (MNV) RdRp. RdRps with mutations at divalent metal ion binding residues did not activate RIG-I signaling. Furthermore, both NoV and MNV RdRp activities were stimulated by the coexpression of their respective VPg proteins, while mutations in the putative site of nucleotide linkage on VPg abolished most of their stimulatory effects. Sequencing of the RNAs linked to VPg revealed that the cellular *trans*-Golgi network protein 2 (TGOLN2) mRNA was the template for VPg-primed RNA synthesis. Small interfering RNA knockdown of RNase L abolished the enhancement of signaling that occurred in the presence of VPg. Finally, the coexpression of each of the other NoV proteins revealed that p48 (also known as NS1-2) and VP1 enhanced and that VP2 reduced the RdRp activity. The assay should be useful for the dissection of the requirements for NoV RNA synthesis as well as the identification of inhibitors of the NoV RdRp.**

Human noroviruses (NoV) (genus *Norovirus*, family *Caliciviridae*) are nonenveloped positive-strand RNA viruses that are responsible for more than 90% of all epidemic viral gastroenteritis outbreaks in the United States (2). At least four epidemics of gastroenteritis took place between 1995 and 2009, with a single genotype, GII.4, associated with these epidemics (9). Noroviruses are also highly contagious, extremely stable in the environment, resistant to common disinfectants, and associated with debilitating illness (33). Research in the development of prevention strategies has been impaired because permissive cell culture systems and robust animal models are lacking for NoV causing human disease.

The NoV genomic RNA is ~7.5 kb, and the genome organization has some similarities to that of the related picornaviruses (Fig. 1A). The genome typically contains three open reading frames (ORFs). ORF2 and ORF3 encode the major and minor structural proteins VP1 and VP2, respectively (60). ORF1, located in the first two-thirds of the genome, encodes an ~200-kDa polyprotein that is proteolytically processed by the virus-encoded 3C-like protease (3C Pro) to yield the nonstructural proteins essential for the establishment of viral replication complexes and genome replication. Of particular note to this work, ORF1 contains NS5, also known as VPg, which is covalently linked to the 5′ end of the genome, and NS7, the RNA-dependent RNA polymerase (RdRp). The key role that the NoV RdRp plays in viral genome replication and the fact that cells lack an equivalent make the RdRp an attractive target for development of norovirus-specific antiviral therapies. The linkage of VPg to viral RNA is thought to occur during viral genome replication whereby VPg is attached as a protein primer to the 5′ terminus of the genomic RNAs (47). Biochemical data confirmed the ability of the NoV RdRp to transfer nucleotides to the VPg (47), and the covalent linkage of VPg to the 5′ end of NoV RNA has been shown to be essential for virus infectivity (24).

Transcripts of the viral genome and double-stranded RNA (dsRNA) replication intermediates synthesized by the viral RdRp in a cell during viral replication are sensed by various innate immune receptors to activate the cellular defenses (62). The retinoic acid-inducible gene I (RIG-I) and the melanoma differentiation-associated gene 5 (MDA5) are the two important cytoplasmic innate immune receptors that contain DExD/H-box motifs characteristic of superfamily II helicases. Both proteins also contain two N-terminal caspase recruitment domains (CARDs), which can interact with a CARD in the adaptor protein, IPS-1 (also known as MAVS, VISA, or Cardif) (67). IPS-1 relays the signal to the kinases TBK1 and IκB kinase ε (IKK-ε), which phosphorylate the transcription factors NF-κB, interferon (IFN) regulatory factor 3 (IRF-3), and IRF-7. These transcription factors subsequently translocate to the nucleus to induce type I IFN expression, which further induces many interferon-stimulated genes (19, 27, 50, 53).

We have developed a cell-based assay for human NoV RdRp (the NoV-5BR assay) that can assess RNAs synthesized by viral RdRps through the activation of RIG-I or MDA5, leading to the production of firefly luciferase from the IFN-β promoter (46). With the NoV-5BR assay format, we demon-

* Corresponding author. Mailing address for C. Kao: Department of Molecular and Cellular Biochemistry, 205C Simon Hall, 212 S. Hawthorne Drive, Indiana University, Bloomington, IN 47405. Phone: (812) 855-7583. Fax: (812) 856-5710. E-mail: ckao@indiana.edu. Mailing address for I. Goodfellow: Imperial College London, St. Mary's Campus, Norfolk Place, London W2 1PG, United Kingdom. Phone: 44 2075942002. Fax: 44 207594 3973. E-mail: I.Goodfellow@Imperial.ac.uk.

▽ Published ahead of print on 12 October 2011.

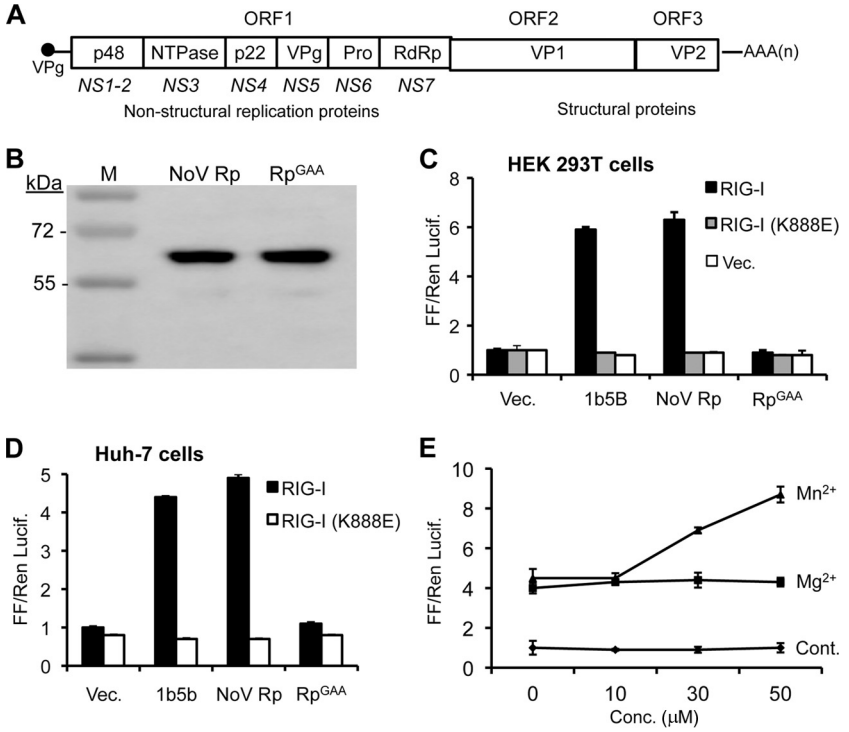


FIG. 1. RNA synthesis-competent NoV RdRp can activate innate immune receptor-mediated signaling. (A) Typical genome organization of human NoV. (B) Western blot of the expression of wild-type or an active site mutant NoV RdRp (norovirus Hu/GII.4/MD-2004/2004/US). Cells transfected to express the FLAG-tagged WT (NoV Rp) or the active site mutant ($Rp^{GAA}$) of the NoV GII.4 RdRp were lysed in sample buffer, resolved with a 4-to-12% bis-Tris gel, and subjected to Western blotting with mouse monoclonal antibody to FLAG tag (Sigma). HRP-coupled rabbit anti-mouse secondary antibody was used to detect the primary antibody, and the signal was developed with the ECL Plus Western blot detection system (Amersham, United Kingdom). The sizes of the relevant molecular weight markers are shown to the left of the Western blot image. (C) Results from the NoV-5BR assay for the NoV RdRp in HEK 293T cells. Plasmids that expressed the proteins are denoted on the *x* axis. 1b5B is the RdRp of HCV genotype 1b. Ratios of firefly to *Renilla* luciferase activities are shown on the *y* axis. The data are the means from three replicates and are representative of three independent experiments, and the standard errors are shown above the bars. (D) Results from a NoV-5BR assay performed in cultured human hepatocytes (Huh-7). The data are the means from three replicates, and the standard errors are shown above the bars. (E) Effects of $Mn^{2+}$ or $Mg^{2+}$ on NoV RdRp activity. The divalent metals were added directly to the medium of the cultured HEK 293T cells. The control reaction monitored the effect of $Mn^{2+}$ on cells that expressed the RIG-I receptor and the two luciferases but not the GII.4 polymerase.

strate that the transiently expressed RdRps from NoV GII.4 and related murine norovirus (MNV) are active for RNA synthesis. In the presence of coexpressed VPg, the NoV RdRp can produce a VPg-primed RNA that can be processed by the cellular endoribonuclease RNase L. Furthermore, the NoV proteins p48, VP1, and VP2 can modulate GII.4 RdRp activity in a species-specific manner.

## MATERIALS AND METHODS

**Plasmid constructs and cell cultures.** Each of the NoV genes, p48 (NS1-2), NTPase (NS3), p22 (NS4), VPg (NS5), Pro (NS6), RdRp (NS7), VP1, and VP2 (norovirus Hu/GII.4/MD-2004/2004/US; GenBank accession number DQ658413), were custom synthesized (Origene). Forward and reverse primers containing AgeI and NheI restriction enzyme sites, respectively, were used to amplify the cDNAs for subcloning into the pUNO vector. NoV RdRp with an N-terminal FLAG tag and NoV VPg with C-terminal FLAG and hemagglutinin (HA) tags were constructed using PCR. p48, NTPase, p22, 3C Pro, VP1, and VP2 had HA tags at their C termini. The sequences of all constructs used in this study were confirmed by use of the BigDye Terminator v3.1 cycle sequencing kit (Applied Biosystems). MNV RdRp and VPg were PCR amplified from a cDNA clone of MNV-1 strain CW1 (GenBank accession number DQ285629.1) (64) and cloned into the pUNO vector (Invivogen Inc.).

Plasmids containing the cDNAs of RIG-I (pUNO-hRIG) and MDA5 (pUNO-hMDA5) were obtained from Invivogen (San Diego, CA). The Toll-like receptor 3 (TLR3) plasmid (pcDNA-TLR3) was previously described by Sun et al. (59). An IFN-β-Luc plasmid containing the firefly luciferase reporter gene driven by the IFN-β promoter gene was used as the reporter plasmid. pRL-TK, expressing *Renilla reniformis* luciferase driven by the herpes simplex virus thymidine kinase (TK) promoter, was used to monitor and standardize the efficacy of transfection (Promega, Madison, WI). For the assay in Huh-7 cells, *Renilla* luciferase driven by a cytomegalovirus promoter was used.

**Dual luciferase reporter assays.** Human embryonic kidney (HEK 293T) cells were cultured in Dulbecco's modified Eagle's medium (DMEM) GlutaMax high-glucose medium (Gibco) containing 10% fetal bovine serum (FBS) at 37°C with 5% $CO_2$. Huh-7 cells were cultured in DMEM GlutaMax low-glucose medium (Gibco) supplemented with 10% FBS and 1× nonessential amino acids.

The 5BR reporter assay was performed as described by Ranjith-Kumar et al. (46). Briefly, plasmids expressing RdRp and VPg were cotransfected along with plasmids to express RIG-I or MDA5, as well as the firefly and *Renilla* luciferase reporters. All transfections in this work used Lipofectamine 2000 according to the manufacturer's instructions (Invitrogen, Carlsbad, CA). At 24 h prior to transfection, $0.5 \times 10^5$ cells were seeded into each well of Costar 96-well plates in DMEM containing 10% FBS. Cells were then typically transfected at 75% confluence. A typical transfection mixture contained 20 ng of pIFN-β-Luc, 5 ng of pRL-TK, 0.5 ng of pUNO-hRIG-I, and 50 ng of the plasmid expressing the viral polymerase. Where necessary, the vector plasmid (pUNO-MCS) was used to maintain a constant amount of plasmid DNA per transfection. At 36 h after transfection, luciferase activity was measured using the Dual-Glo luciferase assay system (Promega, Madison, WI) and a Synergy 2 microplate reader (BioTek,

Winooski, VT). The ratios of firefly luciferase to *Renilla* luciferase activities are shown below in Results unless stated otherwise.

When used, the exogenous RIG-I agonist was a 60-nucleotide (nt) hairpin triphosphorylated RNA (shR9) and was transfected at a 10 nM final concentration into cells. The TLR3 assay was performed as described by Ranjith-Kumar et al. (45) using IFN-stimulated response element (ISRE)–Luc as the firefly reporter plasmid. TLR3-expressing cells were induced with poly(I:C) (500 ng/ml; Amersham Biosciences). The cells were assayed for luciferase levels 18 to 22 h after transfection of exogenous agonists.

**Protein expression analysis.** 293T cells ($1.0 \times 10^5$ cells per well) were transfected with 100 ng of each plasmid in a 48-well cell culture plate (BD Falcon). After 24 h of transfection, cells were washed once with 1× phosphate-buffered saline (PBS; pH 7.4) and harvested by gentle scraping into 1× SDS-PAGE sample buffer. Cell lysates were resolved on a 4-to-12% NuPAGE Novex bis-Tris gel and transferred to polyvinylidene difluoride (PVDF) membranes (Invitrogen, Carlsbad, CA). Membranes were blocked with 5% nonfat milk in TBS-T (Tris-buffered saline–Tween 20) for 2 h and incubated overnight in blocking buffer supplemented with the respective primary antibody. Following washes in TBS-T, membranes were incubated in blocking buffer supplemented with horseradish peroxidase (HRP)-conjugated secondary antibody and developed using the ECL Plus detection system (Amersham, United Kingdom). NoV RdRp and VPg were detected by using a mouse monoclonal anti-FLAG monoclonal antibody (Sigma Inc., St. Louis, MO). RNase L was detected with anti-RNase L mouse monoclonal antibody (Millipore, Bedford, MA), and β-actin was detected with anti-β-actin mouse monoclonal antibody (Santa Cruz Biotechnology, Santa Cruz, CA). Expression analysis of MNV NS7 protein and glyceraldehyde-3-phosphate dehydrogenase used rabbit polyclonal antibodies (Ambion, Austin, TX). The blots were subsequently probed with goat anti-mouse DyLight 680 and goat anti-rabbit DyLight800 (Thermo Scientific) before reading the results in a Licor Odyssey.

**Electrophoretic mobility shift assays and VPg-linked RNA sequencing.** To examine the VPg-linked RNAs, 293T cells ($1.0 \times 10^6$) were seeded in each well of 6-well cell culture plates (BD Falcon), and 1 μg of recombinant plasmid expressing FLAG-tagged RdRp was cotransfected with 100 ng of recombinant plasmid expressing HA-tagged VPg. At 24 h later, total RNA, along with any covalently linked VPg, were isolated using a Qiagen RNeasy minikit. The RNA preparations were subsequently resolved with 4-to-12% NuPAGE Novex bis-Tris gel and morpholinepropanesulfonic acid-SDS running buffer (Invitrogen, Carlsbad, CA) and transferred to PVDF membranes, and the VPg linked to RNAs was detected by Western blotting using an anti-HA antibody.

The RNAs linked to VPg were purified and prepared for DNA sequencing as follows. VPg was immunoprecipitated using anti-HA tag polyclonal antibody covalently linked to Dynabeads M-270 epoxy resin. An RNA adapter (5′-AUC GUAUGCCGUCUUCUGCUUGU-3′) was ligated to the 3′ end of VPg-linked RNAs, digested with proteinase K to remove VPg linked to RNA, extracted with a 1:1 phenol-chloroform mixture followed by ethanol precipitation. First-strand cDNAs were synthesized using a specific reverse primer that recognizes the 3′ adapter sequence (5′-CAAGCAGAAGACGGCATAC-3′) and SuperScript III reverse transcriptase (Invitrogen). Second-strand cDNAs were synthesized using *Escherichia coli* RNase H (New England BioLabs [NEB]) and *E. coli* DNA polymerase I (NEB), as described by Gubler and Hofman (23). The cDNAs were treated with T4 DNA polymerase (NEB) and tailed with *Taq* DNA polymerase (NEB), prior to cloning into a TOPO 2.1 PCR vector (Invitrogen). Plasmids with inserts were sequenced using the BigDye Terminator v3.1 cycle sequencing kit (Applied Biosystems).

**Northern hybridization.** Northern blots were probed using the methods of Sambrook and Russell (49). The probe was an oligonucleotide corresponding to the sense strand of the the *trans*-Golgi network protein 2 (TGOLN2) sequence (5′-CTGACCTCATTTCTCCCCCGCAGGAGGAAG-3′) radiolabeled with T4 polynucleotide kinase and [γ-$^{32}$P]ATP (NEB), and the radioactive signal was imaged using a Typhoon 9210 variable mode imager (Amersham Biosciences).

**Knockdown of RNase L.** HEK 293T cells seeded at $0.5 \times 10^5$ cells/well in a 96-well plate were transfected 5 to 6 h postseeding with 10, 50, and 100 nM RNase L-specific small interfering RNA (siRNA; Invitrogen) or control siRNAs. At 48 h after siRNA transfection, the cells were transfected with either empty vector or with plasmids expressing NoV RdRp, VPg, pRL-TK, and IFN-β-Luc. Dual-luciferase quantification was performed at 24 h posttransfection.

**Murine norovirus reverse genetics recovery.** Reverse genetics recovery of MNV was performed essentially as previously described using the plasmid pT7MNV-3′Rz containing the MNV CW1 genome under the control of the T7 RNA polymerase promoter (14). BHK21 cells were infected with fowlpox virus expressing T7 RNA polymerase (14) and subsequently transfected with 1 μg of cDNA clone by using Lipofectamine 2000 (Invitrogen). At 24 h posttransfection the infectious virus was released by freeze-thawing the samples, and the virus was titrated based on the 50% tissue culture infective dose in RAW 264.7 cells.

## RESULTS

**RNAs synthesized by NoV RdRp can induce signaling by RIG-I.** We sought to establish a cell-based assay to examine RNA synthesis by the human NoV based on the 5BR assay format, which has been used to detect the RNAs made by the hepatitis C virus (HCV) RdRp (46). An expression vector that contained the NS7 cDNA coding region of NoV GII.4 was constructed along with a mutant NS7 in which the active site GDD residues were changed to GAA ($Rp^{GAA}$). Western blotting confirmed that both the wild-type (WT) and the $Rp^{GAA}$ mutant RdRps were expressed and to comparable levels (Fig. 1B). For our assays, we expressed at least four constructs in cells: the viral RdRp to produce RNAs, RIG-I to detect RdRp products, a firefly luciferase construct driven by the IFN-β promoter that can be activated by the RNA-bound RIG-I, and a *Renilla* luciferase driven by the RIG-I-insensitive TK promoter to serve as an internal control. The ratios of the two luciferases thus indirectly reported on the RNA products made by the NoV RdRp. In multiple experiments, a 4- to 8-fold increase in the firefly luciferase activity was observed when the cells expressed the WT NoV RdRp, similar to the levels observed with an HCV genotype 1b NS5B RdRp (Fig. 1C). This increase was not observed with the $Rp^{GAA}$ mutant (Fig. 1C). These results suggest that the NoV-5BR assay can detect RNAs synthesized by the NoV RdRp.

The reactions conditions for the NoV-5BR assay have been optimized. The concentration of the plasmid encoding GII.4 RdRp with the highest signal-to-background ratio was approximately 50 ng, and the optimal time to assess luciferase levels was 36 h after plasmid transfection (data not shown). Furthermore, comparable results were observed in assays performed with 293T and Huh-7 cells (Fig. 1C and D). A mutant RIG-I defective in ligand binding (K888E [37]) resulted in only background levels of firefly luciferase activity from the IFN-β promoter (Fig. 1C). These results demonstrate that RIG-I binding of the RNAs produced by the NoV RdRp is required for the observed luciferase reporter production.

The NoV RdRp can initiate RNA synthesis by a *de novo* mechanism in biochemical assays in the absence of VPg (10, 47). Furthermore, *de novo*-initiated RNA synthesis by the NoV RdRp *in vitro* can be increased by adding $Mn^{2+}$ to the reaction buffer (47). We found that supplementing the medium of cells with up to 50 μM $MnCl_2$ increased luciferase levels by 4-fold without an effect on *Renilla* luciferase levels (Fig. 1E). Higher levels of $Mn^{2+}$ caused cytotoxicity, consistent with reports by Ranjith-Kumar et al. (46). $MgCl_2$ added to the medium at up to 200 μM had no effect on the output from the NoV-5BR assays (Fig. 1E). The results with the activation of RIG-I and the effects of $Mn^{2+}$ are consistent with the GII.4 RdRp utilizing *de novo*-initiated RNA synthesis in the absence of the VPg protein.

**The NoV RdRp can activate signaling by MDA5, but not by TLR3.** We next aimed to determine whether other innate immune receptors could substitute for RIG-I in the NoV-5BR assay. MDA5 is a member of the RIG-I-like receptor family that responds to longer dsRNAs than does RIG-I (35). Re-

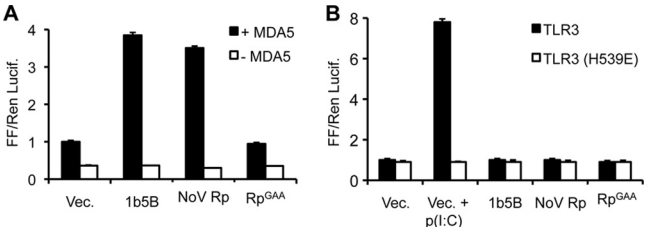


FIG. 2. MDA5, but not TLR3, can replace RIG-I in the NoV-5BR assay. (A) The NoV RdRp can signal through MDA5 in 293T cells. 1b5B is the RdRp from HCV. $Rp^{GAA}$ is an active site mutant of the NoV RdRp. (B) TLR3 signaling was not activated by the products of the NoV RdRp. A TLR3 mutant defective in ligand binding, H539E, served as a control to illustrate signaling that was dependent on the WT TLR3. pI:C denotes poly(I:C), a TLR3 agonist, which was added to the medium of cells to a final concentration of 500 ng/ml.

placing RIG-I with MDA5 also led to signaling in the presence of catalytically active NoV RdRp, but not by an active site mutant of the NoV RdRp (Fig. 2A). The level of luciferase activity through MDA5 was usually lower than through RIG-I. The activation of both RIG-I and MDA5 suggests that at least some RNAs synthesized by the NoV RdRp have the length and terminal modifications for recognition by either receptor.

No increase in luciferase production was observed with the innate immune receptor TLR3, which signals from acidic endosomes (Fig. 2B) (36). In these cells, TLR3 did respond to exogenously provided poly(I:C) ligand but not to catalytically active NoV RdRp. A TLR3 mutant defective in ligand binding, H539E, did not respond to poly(I:C), and since TLR3 detects ligands in endosomes (36), the NoV RdRp products may not gain access to endosomes to induce TLR3 signaling.

**Assay for murine norovirus RdRp activity.** MNV is the only fully infectious system currently available for any NoV and for which reverse genetic systems exist (14, 61). Having a parallel 5BR assay for the MNV RdRp could generate results that can be examined in an infectious virus system. In addition, having assays for both the MNV and NoV RdRps will allow us to determine whether requirements for RNA synthesis are specific to a polymerase. The WT and the active site mutant MNV RdRps were constructed, and both were determined to express at comparable levels in Western blot assays (Fig. 3A). However, only the WT MNV RdRp was able to activate reporter expression, to levels comparable to those from the NoV GII.4 RdRp (Fig. 3B).

NoV RNA synthesis during infection requires the protein primer VPg (47). To examine whether our assay could detect

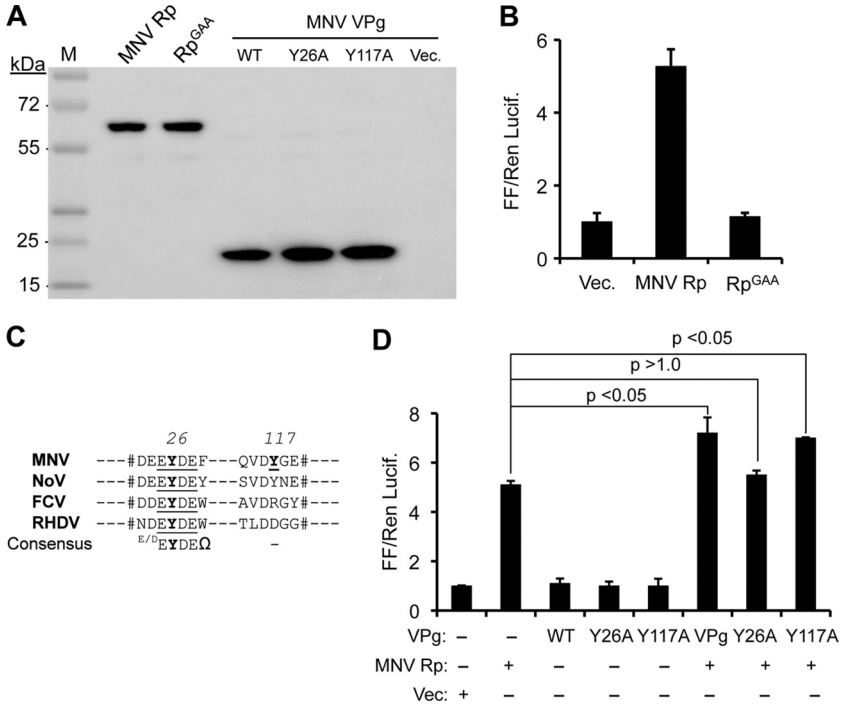


FIG. 3. RNA synthesis-competent MNV RdRp can activate innate immune receptor-mediated signaling. (A) Western blot of the FLAG-tagged MNV proteins produced in HEK 293T cells. A monoclonal antibody recognizing the FLAG epitope was used to detect the MNV RdRp and VPg proteins. HRP-coupled rabbit anti-mouse secondary antibody was used to detect the primary antibody, and the signal was developed with the ECL Plus Western blot detection system (Amersham, United Kingdom). (B) WT MNV RdRp can induce RIG-I signaling in HEK 293T cells. $Rp^{GAA}$ is the active site mutant of MNV RdRp. (C) Sequence alignment of VPg proteins from representative members of the *Caliciviridae*. The predicted site of RNA linkage in the calicivirus VPg is highlighted in bold. Tyr26 is the site of nucleotidylylation in MNV VPg, while the site in NoV corresponds to Tyr27. Tyr117 of the MNV VPg protein, reported to be important for nucleotidylylation *in vitro*, is also highlighted in bold. The conserved signature motif of the calicivirus VPg proteins is shown (E/DE**Y**DEΩ). (D) Effects of coexpressed wild-type or mutant VPgs on the activity of the MNV polymerase. The presence of a plasmid used in the transfection of HEK 293T cells is shown by a plus symbol below the *x* axis. A plus symbol in the row titled "Vec" denotes that an empty vector was transfected into the cells. The data are the means from three replicates and are representative of three independent experiments, and the standard errors are shown above the bars. *P* values less than 0.05 were considered statistically significant.

the effect of VPg, we coexpressed the MNV RdRp along with the MNV VPg. Based on sequence homology and also previously described reports on other caliciviruses (8, 14, 42), Y26 of MNV VPg is the most likely site for the linkage to viral RNA (Fig. 3C). However, Y117 has been reported to prime RNA synthesis in biochemical assays (25). Therefore, we made the Y26A and Y117A mutant VPgs and coexpressed them with the MNV polymerase. The WT and mutant VPgs were expressed to comparable levels in Western blot assays (Fig. 3A). In the presence of the WT VPg or the Y117A mutant, we consistently observed statistically significant ($P < 0.05$) enhancement of luciferase levels, but not with the Y26A mutant (Fig. 3D). These results suggest that Y26 of the MNV VPg is important for the interaction with the MNV RdRp.

A functional interaction between the MNV VPg and RdRp in the 5BR assay format should allow us to determine whether the interaction mimics the requirement in MNV infection. Therefore, conservative substitutions at Y26 or Y117 were engineered into an infectious MNV cDNA clone, and the effects of the mutations on virus recovery were examined using a fowlpox virus-based reverse genetics system previously described (14). The RdRp levels observed upon transfection of the cDNA clones were similar, indicating that the mutations did not affect polyprotein expression (Fig. 4A). However, while the Y26 substitution ablated virus recovery by at least 4 logs and produced no plaques, the Y117 mutant resulted in viral titers and plaque morphologies similar to those of the wild-type virus (Fig. 4B and C). These results demonstrate that the NoV-5BR assay can recapitulate the requirements for VPg in MNV RNA synthesis. Furthermore, in contrast to published *in vitro* observations, linkage of VPg through Y117 to viral RNA is not likely to be relevant in MNV infection.

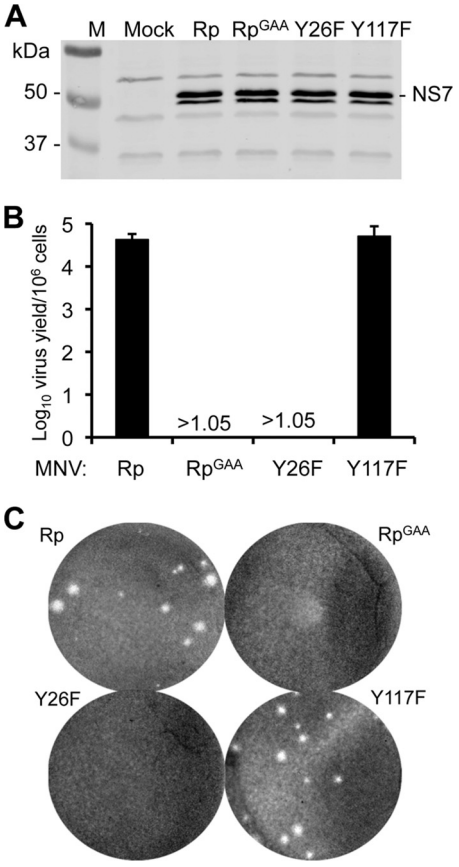


FIG. 4. Y26 of the MNV VPg is required for successful MNV infection. (A) Virus yield following fowlpox virus-mediated reverse genetics recovery from cDNA constructs of either wild-type MNV (Rp), RdRp active site mutant ($Rp^{GAA}$), or constructs containing the mutations Y26F or Y117F in VPg. Baby hamster kidney cells previously infected with fowlpox virus expressing T7 RNA polymerase were transfected with each of the cDNA clones. At 24 h posttransfection the cultures were freeze-thawed, and the virus yields were determined in permissive RAW 264.7 cells. (B) Western blot of MNV proteins from BHK21 cells. One microgram of each MNV cDNA clone was transfected using Lipofectamine 2000 (Invitrogen) into the cells infected with fowlpox virus expressing T7 RNA polymerase. At 24 h posttransfection samples were separated by SDS-PAGE, transferred to nitrocellulose, and probed with rabbit polyclonal anti-NS7. Antibody binding was detected with goat anti-rabbit DyLight800 conjugate (Thermo Scientific) before results were read with a Licor Odyssey apparatus. (C) Virus titer and plaque phenotype of the viruses recovered in the experiment described for panel A.

**VPg-primed RNA synthesis by the NoV RdRp.** We sought to determine whether the VPg protein of the GII.4 virus could enhance the activity of the GII.4 RdRp. The WT NoV VPg or a Y27A variant, the presumed site of nucleotide addition (4), were coexpressed along with the NoV RdRp. The WT VPg reproducibly enhanced reporter output by up to 3-fold above levels in assays performed with the RdRp alone ($P < 0.05$), while Y27A did not, despite the two VPg proteins being expressed at similar levels (Fig. 5A and B). The enhancement was also proportional to the concentration of the VPg-expressing plasmid transfected into the cells (data not shown). These results mirror those from the MNV VPg and RdRp and demonstrate that the GII.4 VPg can also enhance NoV GII.4 RdRp activity.

To determine whether the VPg-dependent enhancement of RdRp activity displayed species-specific selectivity, we performed a mix-and-match experiment. When the NoV VPg was coexpressed with MNV polymerase, and vice versa, enhancements in the heterologous pairings were not statistically significant ($P > 0.5$), compared with homologous pairings, which had $P$ values of $<0.05$ (Fig. 5B). Furthermore, no stimulatory effects of VPg were observed with the RdRps of the HCV and the Brome mosaic virus (BMV), which are also active in the 5BR assay format (Fig. 5C) (46), demonstrating that the effects of the VPg were due to species-specific interactions between the VPg and RdRp of the noroviruses.

The stimulatory effect of VPg could be due to increased RNA synthesis by the RdRp in the presence of VPg, increased stability of the VPg-primed RNA, or more efficient induction of RIG-I signaling. We first examined whether VPg-primed RNA could be detected by immunoprecipitating the HA-tagged VPg, and we analyzed the products by Western blotting. A portion of the VPg was found to exist in a higher-molecular-weight form only in the presence of the WT NoV RdRp, but not with an active site mutant (Fig. 6A), suggesting the VPg does indeed prime RNA synthesis by the RdRp. To confirm this, we selectively purified total RNA from cells coexpressing the VPg with either WT or catalytically inactive RdRp and probed by Western blotting to detect VPg as described previously (13). VPg copurified with the RNAs when it was coexpressed with the WT RdRp, but not with active site mutant

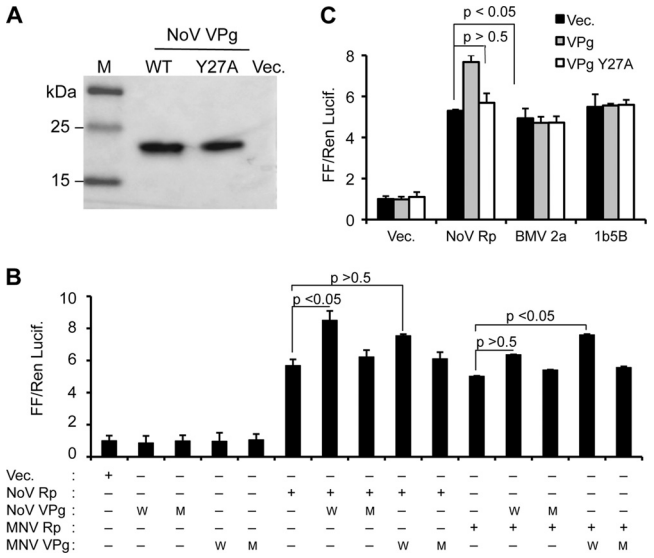


FIG. 5. Effects of coexpressed VPg on NoV GII.4 RdRp activity. (A) Western blot showing that the NoV VPg WT and the Y27A mutant proteins are expressed to comparable levels. (B) Effects of NoV and MNV VPgs on homologous and heterologous combinations of the NoV or MNV RdRps. W, WT VPg; M, mutant VPg. A plus symbol below the *x* axis shows the presence of the respective plasmids used in the transfection of the HEK 293T cells. The data are the means from three replicates and are representative of three independent experiments, and the standard errors are shown above the bars. Statistical analysis was performed by using the pairwise Student *t* test, and the *P* values are shown above the samples that were compared. (C) The NoV VPg does not enhance the activities of the 1b HCV RdRp or the BMV 2a RdRp in transiently transfected HEK 293T cells. The data are the means from three replicates and are representative of two independent experiments, and the standard errors are shown above the bars. Statistical analysis was performed by using the pairwise Student *t* test. The difference between the NoV Rp and NoV Rp+VPg was statistically significant ($P < 0.05$).

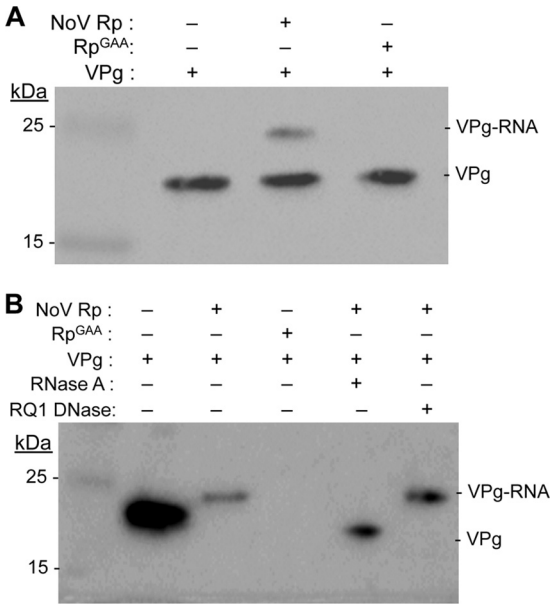


FIG. 6. VPg-primed RNA synthesis in the presence of NoV RdRp. (A) Western blot analysis of VPg immunoprecipitated from HEK 293T cells expressing the WT (NoV Rp) or mutant RdRp ($Rp^{GAA}$) and WT VPg (VPg) proteins. A plus symbol denotes addition of the corresponding plasmid. The samples were resolved on a 4-to-12% denaturing PAGE gel prior to Western blotting with anti-HA antibodies. The relevant masses from the standards are shown to the left of the Western blot image. The identities of the molecules are shown to the right of the Western blot image. VPg-RNA, VPg linked to RNA; VPg, free VPg. (B) Western blotting results for the total RNAs purified from HEK 293T cells that expressed either the WT or mutant RdRp and VPg proteins. The RNAs were electrophoresed in a 4-to-12% denaturing PAGE gel. A plus symbol in the rows labeled RNase A or RQ1 DNase denotes a 30-min treatment with a 10-μg final concentration or 5 units, respectively, of the appropriate enzyme prior to loading the sample for SDS-PAGE. VPg-RNA, VPg linked to RNA; VPg, free VPg. Lane 2 contains free VPg generated from cells transfected to produce only VPg and was loaded to serve as a molecular mass marker.

(Fig. 6B). When an aliquot of the above sample was treated with RNase A, the VPg shifted to a lower-molecular-weight form (Fig. 6B). Treatment with RQ1 DNase did not cause VPg to shift to a lower-molecular-weight form (Fig. 6B). Along with the data in Fig. 1E and 3C, we conclude that the NoV RdRp can perform *de novo*-initiated RNA synthesis as well as VPg-dependent RNA synthesis. This could mimic the distinct requirements for plus- and minus-strand RNA synthesis, the latter of which does not require VPg (10, 47).

**VPg-linked RNA recognition by RIG-I involves RNase L processing.** The attachment of VPg to the 5′ end of RNA will remove the 5′-triphosphate in the RdRp products, one of the features recognized by RIG-I to activate innate immune signaling (28). The fact that RIG-I can respond to the RNAs made in the presence of VPg raises questions about ligand recognition by RIG-I. RIG-I also recognizes viral RNAs processed at their 3′ terminus by the endoribonuclease RNase L, which leaves a 3′-phosphate in the RNA (40, 41). Therefore, we examined whether RNase L can process VPg-linked RNAs in the context of the NoV-5BR assay. Knockdown of RNase L with 50 and 100 nM siRNA resulted in a decrease in RNase L levels to 23% and 10%, respectively, as determined by Western blotting (Fig. 7A). The knockdowns had no obvious effect on the assays performed with only the NoV RdRp or with RIG-I that was activated with either a triphosphorylated RNA (shR9) or a dsRNA derived from reovirus (S4dsRNA). However, knockdown of RNase L significantly decreased the level of signaling in cells enhanced by VPg (Fig. 7B). The decrease was to the level of the signal observed with only the NoV RdRp, suggesting that the detection of *de novo*-initiated RNA synthesis by the NoV RdRp was not affected by RNase L. These results indicated that RNase L can process the VPg-primed RNA products in the context of the 5BR assay and that the NoV RdRp can produce *de novo*-initiated RNAs even in the presence of the coexpressed VPg.

To examine further the effect of RNase L knockdown on VPg-linked RNA processing, we immunoprecipitated epitope-tagged VPg and possible RNAs in cells that were subjected to RNase L knockdown. Western blot analysis showed that the quantity of RNA-linked VPg increased as the RNase L levels decreased. There was also a corresponding change in the pool of free VPg concentration in the cells (Fig. 7C). The analysis was also performed with total RNA purified from transiently transfected cells that were subjected to Western blot analysis. Consistent with the results from the immunoprecipitation assay, the quantity of RNA-linked VPg was inversely related to

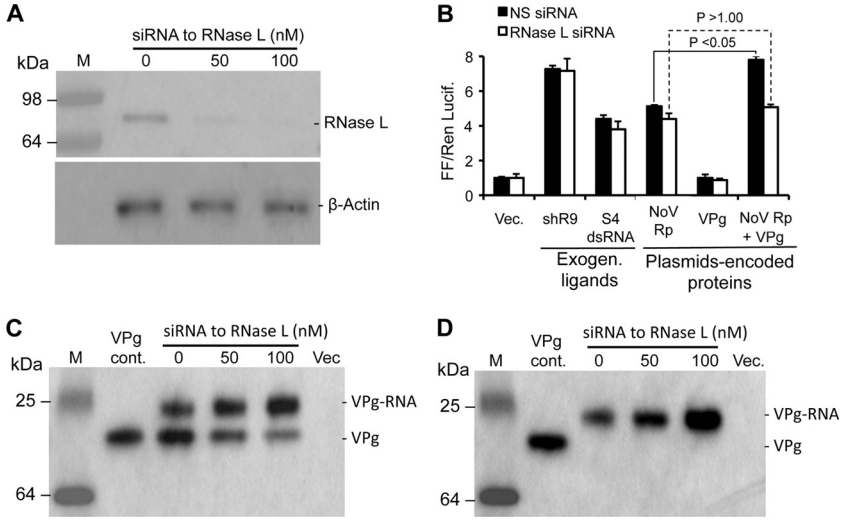


FIG. 7. RNase L participates in the processing of the VPg-primed RNA products synthesized by the NoV RdRp in the NoV-5BR assay. (A) siRNA knockdown of RNase L decreased the levels of RNase L protein in HEK 293T cells. The cells were treated for 48 h with the concentrations of the siRNAs shown above the Western blot image. Twenty microliters of the cell lysate was then subjected to electrophoresis through a 4-to-12% denaturing PAGE gel. The blot was probed with antibodies to RNase L or β-actin, as shown to the right of the Western blot image. (B) Effects of RNase L knockdown on RIG-I signaling with exogenously supplied ligands or ligands produced by the NoV RdRp. The exogenously provided ligands were shR9 and S4dsRNA, produced by *in vitro* transcription using the T7 RNA polymerase and transfected into the cells using Lipofectamine. The NoV RdRp and VPg were transiently expressed from transfected plasmids. NS siRNA, a control, nonspecific siRNA (Invitrogen). The data are the means from three replicates and are representative of two independent experiments, and the standard errors are shown above the bars. Statistical analysis was performed by using the pairwise Student *t* test, and the *P* values are above the samples that were compared. (C) Knockdown of RNase L increased the abundance of the VPg-RNA complex made by the NoV RdRp. The Western blotting results are from immunoprecipitation reactions of cell lysates that expressed the NoV VPg without or with the NoV RdRp probed to detect the VPg protein. The lane VPg alone served as a molecular mass control for free VPg. (D) Confirmation of the effect of RNase L on the abundance of the VPg-RNA complex. Samples shown were used in the Western blot assay containing total RNAs purified from cells that were transfected to expressed the NoV RdRp and VPg after RNase L knockdown. The lane labeled VPg alone served as a molecular mass control for VPg that was not covalently linked to RNA. This species of VPg would not be present in the affinity purification of RNA.

levels of RNase L knockdown (Fig. 7D). All of the above findings suggest that RNase L plays a role in the processing of VPg-linked RNA products of the NoV RdRp and that this processing is required for the stimulation of the IFN-β promoter-based luciferase production in the NoV-5BR assay.

**The NoV RdRp can use a cellular RNA as template for VPg-primed RNA synthesis.** The template used for the synthesis of VPg-linked RNA in cells expressing the NoV RdRp could either have been from the transfected plasmids, as they contain various regions of the NoV genome, presumably any potential *cis*-acting RNA signals or cellular RNAs. To identify the template, we immunoprecipitated the epitope-tagged VPg from cells that coexpressed either the wild type or an active site mutant of the NoV RdRp. The precipitated RNA(s) was subjected to cDNA synthesis followed by cloning and sequencing of 15 clones from two independent experiments. The 15 sequences represented 10 distinct cDNAs of between 39 and 49 nt in length, but all were complementary to the same sequence within the protein-coding region of TGOLN2 mRNA (Fig. 8A). The cDNAs contained two subsets of sequences from contiguous regions of the TGOLN2 mRNA. No RNAs that matched the sequence we used to produce the RdRp or VPg were detected in our analysis. These results show that the NoV RdRp can use a specific cellular mRNA as template for VPg-primed RNA synthesis in the NoV-5BR assay.

To confirm that TGOLN2 was a template for RNA synthesis by the NoV RdRp, we subjected the precipitated VPg from cells expressing the NoV RdRp to a Northern blot assay with a radiolabeled oligonucleotide that corresponds to the TGOLN2 mRNA. Only the cells expressing NoV RdRp competent for RNA synthesis in the presence of the WT VPg revealed products detected by the probe. The VPg samples pretreated with RNase A, but not with RQ1 DNase, abolished recognition by the oligonucleotide probe (Fig. 8B). These results suggest that the VPg is linked to RNA and the sequences are complementary to TGOLN2 mRNA.

**Effect of other NoV proteins on RdRp activity.** The results with VPg encouraged us to examine whether other NoV proteins affect the activity of the NoV RdRp. The expression of all of the proteins in 293T cells was detected by Western blotting using the anti-HA antibody (Fig. 9A). Notably, a minor portion of VP2 migrated as higher-molecular-weight forms, consistent with a previous observation with VP2 expressed from baculovirus vectors (22). When coexpressed with the GII.4 RdRp, we observed that p48, NTPase, p22, and the 3C Pro reduced the internal control *Renilla* levels by more than 20% when plasmid concentrations in excess of 10 ng were used. No apparent cytotoxicity was observed with the VP1 and VP2 proteins. Therefore, all assays were performed with up to 10 ng of the transfected plasmids to reduce toxicity from the GII.4 nonstructural proteins.

All of the nonstructural proteins as well as major structural protein VP1 increased RIG-I-dependent signaling to various degrees relative to the cells expressing the GII.4 RdRp alone,

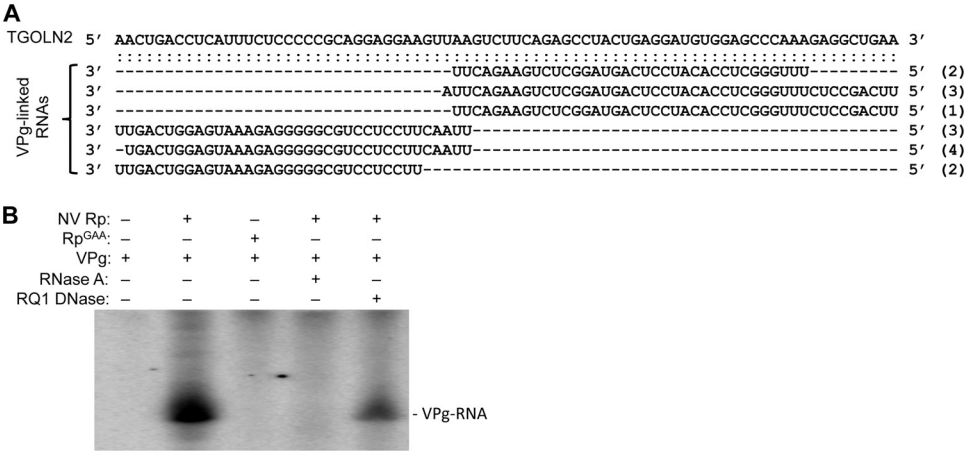


FIG. 8. Identification of a template for VPg-primed RNA synthesis in HEK 293T cells. (A) Alignment of the sequences of the cDNAs derived from the VPg-primed RNAs. The sequence from the cellular TGOLN2 mRNA is shown on the top line in the 5′-to-3′ direction, and the sequences of VPg-linked RNAs are complementary to and shown below the TGOLN2 mRNA in the 3′-to-5′ direction. Each sequence was from an independent cDNA clone, and the numbers in parentheses represent the number of independent sequences obtained. Dashes denote that the sequence was not present. (B) Northern blot of the VPg-RNA complexes immunoprecipitated from HEK 293T cells expressing the WT or mutant RdRp and VPg, performed with a radiolabeled oligodeoxyribonucleotide corresponding to the TGOLN2 mRNA sequence. Where RNase A or RQ1 DNase treatment was used, the immunoprecipitated material was incubated with the enzyme for 30 min prior to electrophoresis on a denaturing PAGE gel.

with p48 and VP1 increasing IFN-β-driven luciferase levels to 160 and 173% of the control (Fig. 9B and C). The values were obtained from six independent samples, and a pairwise *t* test showed that the difference in the luciferase levels was statistically significant ($P < 0.05$). VP2 decreased the RdRp activity to 68% of the vector control ($P < 0.05$). Coexpression of the other proteins with the RdRp did not result in statically significant differences from cells expressing the RdRp and the empty vector ($P > 0.5$). Furthermore, none of the proteins, including the RdRp, altered RIG-I signaling induced by the RIG-I agonist shR9, demonstrating that the proteins do not act through RIG-I (data not shown).

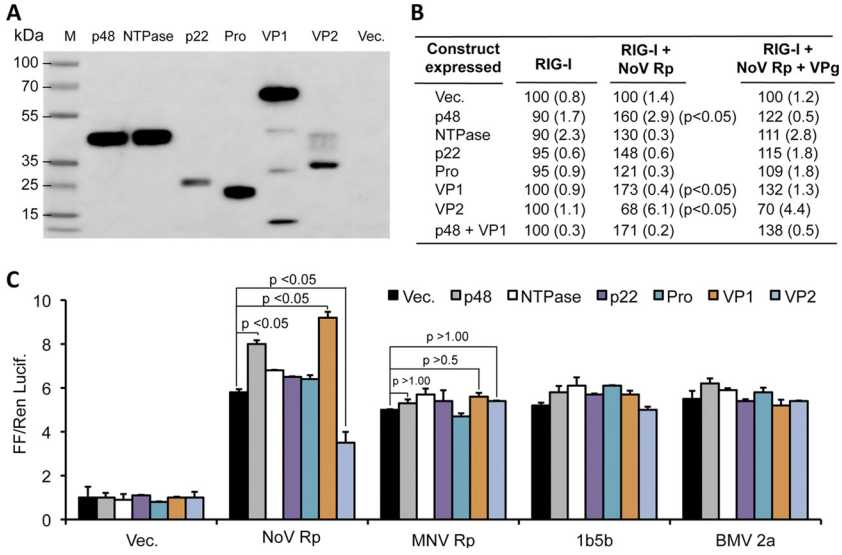


| Construct expressed | RIG-I | RIG-I + NoV Rp | RIG-I + NoV Rp + VPg |
|---|---|---|---|
| Vec. | 100 (0.8) | 100 (1.4) | 100 (1.2) |
| p48 | 90 (1.7) | 160 (2.9) (p<0.05) | 122 (0.5) |
| NTPase | 90 (2.3) | 130 (0.3) | 111 (2.8) |
| p22 | 95 (0.6) | 148 (0.6) | 115 (1.8) |
| Pro | 95 (0.9) | 121 (0.3) | 109 (1.8) |
| VP1 | 100 (0.9) | 173 (0.4) (p<0.05) | 132 (1.3) |
| VP2 | 100 (1.1) | 68 (6.1) (p<0.05) | 70 (4.4) |
| p48 + VP1 | 100 (0.3) | 171 (0.2) | 138 (0.5) |

FIG. 9. Effects of other NoV proteins on RdRp activity. (A) Western blotting of the NoV proteins showed their expression in HEK 293T cells. All of the proteins were HA tagged at their C termini and detected with the goat anti-HA antibody and an HRP-conjugated mouse anti-goat antibody. (B) Summary of the effects of coexpressed NoV GII.4 structural and nonstructural proteins on RIG-I signaling or NoV RdRp activity. Plasmid carrying NoV RdRp was transfected at 50 ng/well, and plasmid carrying each other protein was transfected at 10 ng/well. All data are presented as the means and standard errors of three replicates from three independent assays. The results are normalized to the vector-only control to better allow comparisons. Results statistically different from that of the vector-alone sample are shown with *P* values in parentheses. (C) Effects of the NoV proteins on the RdRps from NoV, MNV, HCV (1b5b), and BMV (BMV 2a). Plasmids encoding all RdRps were transfected into HEK 293T cells at 50 ng, and the plasmids that express the other NoV GII.4 proteins were transfected at 10 ng. Each bar represents the means and standard errors of three replicates from two independent assays. Statistical analysis was performed by using the pairwise Student *t* test, and the *P* values are indicated above the samples that were compared.

We also examined the effects of coexpressed individual NoV proteins on the activities of NoV RdRp in the presence of VPg. While expressing both RdRp and VPg increased the RdRp activity by an additional 1.5- to 3.0-fold, as expected, expression of additional GII.4 proteins did not change the trends seen with the RdRp alone (Fig. 9B, third and fourth columns). These results suggest that any effects of the GII.4 proteins are likely through the RdRp, rather than the RdRp-VPg complex.

To determine whether the modulatory effects of GII.4 proteins were specific to the GII.4 RdRp, each of the proteins was coexpressed with the RdRps from GII.4, MNV, HCV, and BMV. The stimulatory effects of p48 or VP1 were significantly higher for the GII.4 RdRp ($P < 0.05$) than for the other RdRps, including the MNV RdRp (Fig. 9C). The inhibitory effect of VP2 was also the most potent for the GII.4 RdRp ($P < 0.05$), and this effect was not observed with the other RdRps ($P > 0.5$). No change in the general trend of the effects was observed when VPg was coexpressed with the other three RdRps (data not shown). These results suggest that the NoV-5BR assay format can be used to further dissect possible regulatory roles of the NoV GII.4 nonstructural and structural proteins when they are expressed in *trans* in relation to each other.

## DISCUSSION

Despite their impact on human health, noroviruses are one of the most poorly characterized families of small RNA viruses. In this study, we developed a cell-based assay, called the NoV-5BR assay, for RNA synthesis by the RdRps of NoV GII.4 and MNV. The assay couples RNA synthesis by the viral RdRps to innate immune signaling and subsequent reporter luciferase production. This assay was used to demonstrate the specific interaction of VPg and RdRp for the NoV GII.4 as well as the MNV. The VPg-primed RNA synthesis by the RdRp remained capable of activating RIG-I signaling, through processing by the cellular endoribonuclease RNase L. We also demonstrated that p48, VP1, and VP2 encoded by NoV GII.4 can modulate its RdRp activity by using this assay.

**RNA synthesis by the NoV RdRp.** There are several lines of evidence suggesting that NoV RdRps can perform both *de novo*-initiated and VPg-primed RNA synthesis in the 5BR assay format. Replication of norovirus genomic RNA involves VPg-primed initiation, and it is likely that production of the antigenomic RNA uses *de novo* initiation (47), suggesting that the NoV RdRp uses two distinct modes of RNA synthesis during infection. The NoV-5BR assay could duplicate both modes of RNA syntheses and mimic the requirements for calicivirus RNA replication (7, 11, 26, 57). The NoV RdRp can synthesize *de novo* RNA products in the NoV-5BR assay in the absence of VPg, and the addition of $Mn^{2+}$, a cofactor known to increase *de novo* initiation *in vitro*, increased the NoV RdRp-dependent luciferase production (Fig. 1E). In previous studies, NoV RdRp activity was found to depend on the presence of $Mg^{2+}$ or $Mn^{2+}$ and $Mn^{2+}$ and has been shown to preferentially enable RNA synthesis by NoV RdRp *in vitro* (3, 10, 21). In our assay a strong preference for $Mn^{2+}$ over $Mg^{2+}$ was observed (Fig. 1E). The requirement for $Mn^{2+}$ and divalent cations is similar to that of the *de novo*-initiated RNA synthesis by the RdRps of poliovirus and rhinovirus 16, two viruses that use protein-primed RNA synthesis during infection (1, 29), as well as RdRps from viruses that use a *de novo* initiation mechanism during replication, such as HCV (31, 38, 44). For the poliovirus $3D^{Pol}$ protein, it has been suggested that $Mn^{2+}$ may influence polymerization through an indirect effect on folding of the enzyme (16). Ng et al. (43) also suggested that $Mn^{2+}$ helps to form an active structure of the rabbit hemorrhagic disease virus (RHDV) polymerase. $Mn^{2+}$ has been reported to enhance replication initiation for a number of viral RdRps, including that from the plant-infecting BMV and those from members of the *Flaviviridae*, likely through induced changes in the RdRp conformation (32, 44). All these observations demonstrate that the assay could be an invaluable tool to study the RNA synthesis activities of NoV RdRps.

Coexpression of the VPg with the RdRp resulted in an enhanced level of RIG-I signaling (Fig. 5B) and produced RNA-linked VPg molecules (Fig. 6). Notably, the maximal enhancement for RdRp-induced RIG-I signaling was with homologous pairs of the VPg and RdRp from GII.4 and MNV, indicating that there is species-specific recognition of the RdRp and VPg. We emphasize that, while VPg-dependent RNA synthesis has been demonstrated, we cannot rule out another mechanism for VPg to enhance signaling in our assay. Notably, VPg plays multiple roles in calicivirus infection. Recent data indicated that VPg may function in the initiation of translation of NoV RNA (17) and may facilitate RNA encapsidation (48). In poliovirus, $3D^{Pol}$ catalyzes the conversion of VPg into VPg-pUpU(OH) through uridylylation, which acts as a primer for cRNA synthesis (58). In the present study we found UU nucleotides at the 3′-end VPg-linked RNAs (Fig. 8A). Based on this observation, we propose that the VPg-UU could be base pairing with AA on the TGOLN2 template mRNA to synthesize cRNA through VPg-primed RNA synthesis, as reported for poliovirus.

Our finding that siRNA to RNase L decreased the signaling of RdRp in the presence of VPg only to the level seen with the RdRp alone suggested that RNase L is involved in VPg-linked RNA processing but not the processing of *de novo*-synthesized RNA products (Fig. 7B). A role for RNase L in mediating antiviral activity has not been demonstrated for noroviruses, to our knowledge. However, there are numerous precedents in the literature (6, 39, 55). Furthermore, results from the sequencing of the RNA linked to VPg (Fig. 8) revealed the UA and UU dinucleotide signature sequences are the preferred cleavage sites for RNase L (20, 65). Determining whether RNase L affects NoV infection will be important, since RNase L not only degrades viral RNAs but also further enhances innate immune signaling through the RIG-I and MDA5 receptors and impacts the inflammatory responses (52).

In the NoV-5BR assay, the stimulatory effects of a nonstructural protein, p48, and the major structural protein VP1, as well as the inhibitory effect of the minor structural protein VP2 on the RdRp, are intriguing. Viral RNA replication requires a membrane-associated multisubunit complex that has a number of modulatory factors to coordinate the rate and kinetics of synthesis as well as to avoid detection by cellular defenses (15, 18, 51, 63). A yeast two-hybrid screen revealed that the feline calicivirus (FCV) ProPol protein interacted with itself, VPg, and VP1. A relatively weak interaction was also observed between ProPol and the minor capsid protein (VP2 equivalent)

encoded by ORF3 (30). The formation of these replication complexes occurs through a network of viral protein interactions as well as between viral and host-cell proteins. The results of the present study with VP1, which enhanced, and VP2, which reduced, RdRp activity are additional examples in the emerging understanding that viral structural proteins will regulate viral RNA synthesis and gene expression as in other RNA viruses (5, 56, 66).

**Future perspectives.** While the results in this work provided several insights into NoV replication, we emphasize that many of the observations will require careful examination in the context of NoV infection. First is the observation that VPg-linked RNA can be processed by RNase L to lead to RIG-I-based activation of IFN-β-dependent luciferase production (Fig. 7). The preliminary indication from our results is that only the VPg-primed RNAs are cleaved by RNase L. Whether this is due to a specific recognition of RNA attached to VPg remains to be determined. A second area that requires additional analysis is the surprising discovery that TGOLN2 mRNA was the only identified message that served as the VPg-primed template from 15 independent clones sequenced. NoV proteins have been shown to affect protein trafficking through the Golgi apparatus (54), and whether TGOLN2 is specifically targeted during NoV infection as a means to modulate trafficking of NoV proteins remains to be examined. A third area that requires additional analysis is the composition and the molecular interactions that occur within the NoV replication complex. The interaction between the GII.4 RdRp and p48 was not previously detected in the FCV orthologs, and the NoV-5BR assay should be useful in dissecting this interaction. Lastly, the NoV-5BR assay could be useful in the identification of NoV RdRp inhibitors. The NoV-5BR assay will be advantageous over biochemical assays, since it does not require purification of the RdRp and will only assess inhibitors that can penetrate cells. The assay is easily adaptable to RdRps from different viral genotypes. This assay should complement the MNV infectious virus systems (14, 61), as well as the various replicon systems that are available to study NoV replication (12, 34).

## ACKNOWLEDGMENTS

We thank our colleagues, especially C. T. Ranjith-Kumar for invaluable discussions during this work and L. Blatt and J. Symons of Alios BioPharma for discussions on RNase L.

The 5BR assay was developed with funds from the National Institute of Allergy and Infectious Diseases (grants 1RO1AI073335 and RA0750150 to C.K.). I.G. is a Wellcome Senior Fellow and acknowledges funding from the Wellcome Trust.

## REFERENCES

1. **Arnold, J. J., S. K. Ghosh, and C. E. Cameron.** 1999. Poliovirus RNA-dependent RNA polymerase (3Dpol). Divalent cation modulation of primer, template, and nucleotide selection. J. Biol. Chem. **274:**37060–37069.
2. **Atmar, R. L., and M. K. Estes.** 2006. The epidemiologic and clinical importance of norovirus infection. Gastroenterol. Clin. North Am. **35:**275–290.
3. **Belliot, G., et al.** 2005. Norovirus proteinase-polymerase and polymerase are both active forms of RNA-dependent RNA polymerase. J. Virol. **79:**2393–2403.
4. **Belliot, G., S. V. Sosnovtsev, K. O. Chang, P. McPhie, and K. Y. Green.** 2008. Nucleotidylylation of the VPg protein of a human norovirus by its proteinase-polymerase precursor protein. Virology **374:**33–49.
5. **Bernardi, A., and P. F. Spahr.** 1972. Nucleotide sequence at the binding site for coat protein on RNA of bacteriophage R17. Proc. Nat. Acad. Sci. U. S. A. **69:**3033–3037.
6. **Bisbal, C., and R. H. Silverman.** 2007. Diverse functions of RNase L and implications in pathology. Biochimie **89:**789–798.
7. **Black, D. N., J. N. Burroughs, T. J. Harris, and F. Brown.** 1978. The structure and replication of calicivirus RNA. Nature **274:**614–615.
8. **Britton, P., et al.** 1996. Expression of bacteriophage T7 RNA polymerase in avian and mammalian cells by a recombinant fowlpox virus. J. Gen. Virol. **77:**963–967.
9. **Bull, R. A., and P. A. White.** 2011. Mechanisms of GII.4 norovirus evolution. Trends Microbiol. **19:**233–240.
10. **Bull, R. A., et al.** 2011. Comparison of the replication properties of murine and human calicivirus RNA-dependent RNA polymerases. Virus Genes **42:**16–27.
11. **Chang, K. O., K. Y. Green, and L. J. Saif.** 2002. Cell-culture propagation of porcine enteric calicivirus mediated by intestinal contents is dependent on the cyclic AMP signaling pathway. Virology **304:**302–310.
12. **Chang, K., S. V. Sosnovtsev, G. Belliot, A. D. King, and K. Y. Green.** 2006. Stable expression of a Norwalk virus RNA replicon in a human hepatoma cell line. Virology **353:**463–473.
13. **Chaudhry, Y., et al.** 2006. Caliciviruses differ in their functional requirements for eIF4F components. J. Biol. Chem. **281:**25315–25325.
14. **Chaudhry, Y., M. A. Skinner, and I. Goodfellow.** 2007. Recovery of genetically defined murine norovirus in tissue culture by using a fowlpox virus expressing T7 RNA polymerase. J. Gen. Virol. **88:**2091–2100.
15. **Chen, J., and P. Ahlquist.** 2000. Brome mosaic virus polymerase-like protein 2a is directed to the endoplasmic reticulum by helicase-like viral protein 1a. J. Virol. **74:**4310–4318.
16. **Crotty, S., et al.** 2003. Manganese-dependent polioviruses caused by mutations within the viral polymerase. J. Virol. **77:**5378–5388.
17. **Daughenbaugh, K. F., C. S. Fraser, J. W. B. Hershey, and M. E. Hardy.** 2003. The genome-linked protein VPg of the Norwalk virus binds eIF3, suggesting its role in translation initiation complex recruitment. EMBO J. **22:**2852–2859.
18. **El-Hage, N., and G. Luo.** 2003. Replication of hepatitis C virus RNA occurs in a membrane-bound replication complex containing nonstructural viral proteins and RNA. J. Gen. Virol. **84:**2761–2769.
19. **Fitzgerald, K. A., et al.** 2003. IKKε and TBK1 are essential components of the IRF3 signaling pathway. Nat. Immunol. **4:**491–496.
20. **Floyd-Smith, G., E. Slattery, and P. Lengyel.** 1981. Interferon action: RNA cleavage pattern of an oligoadenylate-dependent endonuclease. Science **212:**1030–1032.
21. **Fukushi, S., et al.** 2004. Poly(A)- and primer-independent RNA polymerase of norovirus. J. Virol. **78:**3889–3896.
22. **Glass, P. J., C. Q. Zeng, and M. K. Estes.** 2003. Two nonoverlapping domains on the norwalk virus open reading frame 3 (ORF3) protein are involved in the formation of the phosphorylated 35K protein and in ORF3-capsid protein interactions. J. Virol. **77:**3569–3577.
23. **Gubler, U., and B. J. Hoffman.** 1983. A simple and very efficient method for generating cDNA libraries. Gene **25:**263–269.
24. **Guix, S., et al.** 2007. Norwalk virus RNA is infectious in mammalian cells. J. Virol. **81:**12238–12248.
25. **Han, K. R., et al.** 2010. Murine norovirus-1 $3D^{pol}$ exhibits RNA-dependent RNA polymerase activity and nucleotidylylates on Tyr of the VPg. J. Gen. Virol. **91:**1713–1722.
26. **Herbert, T. P., I. Brierley, and T. D. Brown.** 1997. Identification of a protein linked to the genomic and subgenomic mRNAs of feline calicivirus and its role in translation. J. Gen. Virol. **78:**1033–1040.
27. **Honda, K., et al.** 2005. IRF-7 is the master regulator of type-I interferon-dependent immune responses. Nature **434:**772–777.
28. **Hornung, V., et al.** 2006. 5′-triphosphate RNA is the ligand for RIG-I. Science **314:**994–997.
29. **Hung, M., C. S. Gibbs, and M. Tsiang.** 2002. Biochemical characterization of rhinovirus RNA-dependent RNA polymerase. Antiviral Res. **56:**99–114.
30. **Kaiser, W. J., Y. Chaudhry, S. V. Sosnovtsev, and I. G. Goodfellow.** 2006. Analysis of protein-protein interactions in the feline calicivirus replication complex. J. Gen. Virol. **87:**363–368.
31. **Kao, C. C., et al.** 2000. Template requirements for RNA synthesis by a recombinant hepatitis C virus RNA-dependent RNA polymerase. J. Virol. **74:**11121–11128.
32. **Kao, C., P. Sighn, and D. Ecker.** 2001. De novo initiation of viral RNA-dependent RNA synthesis. Virology **287:**251–260.
33. **Karst, S. M.** 2010. Pathogenesis of noroviruses, emerging RNA viruses. Viruses **2:**748–781.
34. **Katayama, K., G. S. Hansman, T. Oka, S. Ogawa, and N. Takeda.** 2006. Investigation of norovirus replication in a human cell line. Arch. Virol. **151:**1291–1308.
35. **Kato, H., et al.** 2008. Length dependent recognition of double-stranded ribonucleic acids by retinoic acid inducible gene-I and melanoma differentiation-associated gene 5. J. Exp. Med. **205:**1601–1610.
36. **Leonard, J. N., et al.** 2008. The TLR3 signaling complex forms by cooperative receptor dimerization. Proc. Natl. Acad. Sci. U. S. A. **105:**258–263.
37. **Lu, C., et al.** 2010. The structural basis of 5′-triphosphate double-stranded RNA recognition by RIG-I C-terminal domain. Structure **18:**1032–1043.
38. **Luo, G., et al.** 2000. De novo initiation of RNA synthesis by the RNA

dependent RNA polymerase (NS5B) of hepatitis C virus. J. Virol. **74:**851–863.
39. **Luthra, P., D. Sun, R. H. Silverman, and B. He.** 2011. Activation of IFN-β expression by a viral mRNA through RNase L and MDA5. Proc. Nat. Acad. Sci. U. S. A. **108:**2118–2123.
40. **Malathi, K., B. Dong, M. Gale, and R. H. Silverman.** 2007. Small self-RNA generated by RNase L amplifies antiviral innate immunity. Nature **448:**816–820.
41. **Malathi, K., et al.** 2010. RNase L releases a small RNA from HCV RNA that refolds into a potent PAMP. RNA **16:**2108–2119.
42. **McCartney, S. A., et al.** 2008. MDA-5 recognition of a murine norovirus. PLoS Pathog. **4:**e1000108.
43. **Ng, K. K., et al.** 2002. Crystal structures of active and inactive conformations of a caliciviral RNA-dependent RNA polymerase. J. Biol. Chem. **277:**1381–1387.
44. **Ranjith-Kumar, C. T., et al.** 2002. Mechanism of de novo initiation by the hepatitis C virus RNA-dependent RNA polymerase: role of divalent metals. J. Virol. **76:**12513–12525.
45. **Ranjith-Kumar, C. T., et al.** 2007. Effects of single nucleotide polymorphisms on Toll-like receptor 3 activity and expression in cultured cells. J. Biol. Chem. **282:**17696–17705.
46. **Ranjith-Kumar, C. T., Y. Wen, N. Baxter, K. Bhardwaj, and C. C. Kao.** 2011. A cell-based assay for RNA synthesis by the HCV polymerase reveals new insights on mechanism of polymerase inhibitors and modulation by NS5A. PLoS One **6:**e22575.
47. **Rohayem, J., I. Robel, K. Jager, U. Scheffler, and W. Rudolph.** 2006. Protein-primed and de novo initiation of RNA synthesis by norovirus $3D^{Pol}$. J. Virol. **80:**7060–7069.
48. **Sadowy, E., M. Milner, and A. L. Haenni.** 2001. Proteins attached to viral genomes are multifunctional. Adv. Virus Res. **57:**185–262.
49. **Sambrook, J., and D. W. Russell.** 2001. Northern hybridization, p. 7.21–7.75. Molecular cloning: a laboratory manual, 3rd ed. Cold Spring Harbor Laboratory Press, Cold Spring Harbor, NY.
50. **Sato, M., et al.** 2000. Distinct and essential roles of transcription factors IRF-3 and IRF-7 in response to viruses for IFN-α/β gene induction. Immunity **13:**539–548.
51. **Schaad, M. C., P. E. Jensen, and J. C. Carrington.** 1997. Formation of plant RNA virus replication complexes on membranes: role of an endoplasmic reticulum-targeted viral protein. EMBO J. **16:**4049–4059.
52. **Schmidt, A., S. Endres, and S. Rothenfusser.** 2011. Pattern recognition of viral nucleic acids by RIG-I-like helicases. J. Mol. Med. **89:**5–12.
53. **Sharma, S., et al.** 2003. Triggering the interferon antiviral response through an IKK-related pathway. Science **300:**1148–1151.
54. **Sharp, T. M., S. Guix, K. Katayama, S. E. Crawford, and M. K. Estes.** 2010. Inhibition of cellular secretion by nonstructural protein P22 requires a mimic of an endoplasmic reticulum export signal. PLoS One **10:**e13130.
55. **Silverman, R. H.** 2007. Viral encounters with 2′,5′-oligoadenylate synthetase and RNase L during the interferon antiviral response. J. Virol. **81:**12720–12729.
56. **Silvestri, L. S., M. A. Tortorici, R. V. D. Carpio, and J. T. Patton.** 2005. Rotavirus glycoprotein NSP4 is a modulator of viral transcription in the infected cell. J. Virol. **79:**15165–15174.
57. **Sosnovtsev, S., and K. Y. Green.** 1995. RNA transcripts derived from a cloned full-length copy of the feline calicivirus genome do not require VPg for infectivity. Virology **210:**383–390.
58. **Steil, B. P., and D. J. Barton.** 2009. Conversion of VPg into VPgpUpUOH before and during poliovirus negative-strand RNA synthesis. J. Virol. **83:**12660–12670.
59. **Sun, J., et al.** 2006. Structural and functional analyses of the human Toll-like receptor 3. Role of glycosylation. J. Biol. Chem. **281:**11144–11151.
60. **Vashist, S., D. Bailey, A. Putics, and I. Goodfellow.** 2009. Model systems for the study of human norovirus biology. Future Virol. **4:**353–367.
61. **Ward, V. K., et al.** 2007. Recovery of infectious murine norovirus using pol II-driven expression of full-length cDNA. Proc. Natl. Acad. Sci. U. S. A. **104:**11050–11055.
62. **Weber, F., F. Wagner, S. B. Rasmussen, R. Hartmann, and S. R. Paludan.** 2006. Double-stranded RNA is produced by positive-strand RNA viruses and DNA viruses but not in detectable amounts by negative-strand RNA viruses. J. Virol. **80:**5059–5064.
63. **Wimmer, E., C. U. T. Hellen, and X. M. Cao.** 1993. Genetics of poliovirus. Annu. Rev. Genet. **27:**353–436.
64. **Wobus, C. E., et al.** 2004. Replication of norovirus in cell culture reveals a tropism for dendritic cells and macrophages. PLoS Biol. **2:**e432.
65. **Wreschner, D. H., J. W. McCauley, J. J. Skehel, and I. M. Kerr.** 1981. Interferon action: sequence specificity of the ppp(A29p)nA-dependent ribonuclease. Nature **289:**414–417.
66. **Yi, G., E. Letteney, C. H. Kim, and C. C. Kao.** 2009. Brome mosaic virus capsid protein regulates accumulation of viral replication proteins by binding to the replicase assembly RNA element. RNA **15:**615–626.
67. **Yoneyama, M., and T. Fujita.** 2009. A recognition and signal transduction by RIG-I-like receptors. Immunol. Rev. **227:**54–65.